Monthly Notices
of the
ROYAL ASTRONOMICAL SOCIETY

Mon. Not. R. Astron. Soc. **410,** 1583–1592 (2011) doi:10.1111/j.1365-2966.2010.17541.x

Radio emission and active galactic nucleus feedback in post-starburst galaxies

Min-Su Shin,[1,2⋆] Michael A. Strauss[2⋆] and Rita Tojeiro[3⋆]

[1]*Department of Astronomy, University of Michigan, Ann Arbor, MI 48109, USA*
[2]*Princeton University Observatory, Peyton Hall, Princeton, NJ 08544-1001, USA*
[3]*Institute of Cosmology and Gravitation, Dennis Sciama Building, Burnaby Road, Portsmouth PO1 3FX*

Accepted 2010 August 15. Received 2010 August 6; in original form 2010 May 14

ABSTRACT

We investigate radio-mode AGN activity among post-starburst galaxies from the Sloan Digital Sky Survey (SDSS) to determine whether AGN feedback may be responsible for the cessation of star formation. Based on radio morphology and radio loudness from the FIRST and NVSS data, we separate objects with radio activity due to an AGN from ongoing residual star formation. Of 513 SDSS galaxies with strong A-star spectra, 12 objects have 21-cm flux density above 1 mJy. These galaxies do not show optical AGN emission lines. Considering that the lifetime of radio emission is much shorter than the typical time-scale of the spectroscopic features of post-starburst galaxies, we conclude that the radio-emitting AGN activity in these objects was triggered after the end of the recent starburst, and thus cannot be an important feedback process to explain the post-starburst phase. The radio luminosities show a positive correlation with total galaxy stellar mass, but not with the mass of recently formed stars. Thus the mechanical power of AGN feedback derived from the radio luminosity is related to old stellar populations dominating the stellar mass, which in turn are related to the masses of central supermassive black holes.

Key words: galaxies: evolution – galaxies: fundamental parameters – galaxies: jets – galaxies: stellar content – radio continuum: general.

1 INTRODUCTION

Various observational facts and theoretical models have suggested that feedback from active galactic nucleus (AGN) activity has a strong impact on galaxy formation and evolution, especially star formation in galaxies (see Bland-Hawthorn, Veilleux & Cecil 2007, for a review). The starburst-AGN connection has been investigated for a broad range of galaxy and AGN types, showing that the mechanism triggering intensive star formation might also cause strong fuelling on to a central supermassive black hole (e.g. Smith, Lonsdale & Lonsdale 1998; Cid Fernandes et al. 2001; Veilleux 2001; Farrah et al. 2003; Rupke, Veilleux & Sanders 2005; Lonsdale, Farrah & Smith 2006; Liu et al. 2009; Trichas et al. 2009). Effects of AGN activity on the interstellar medium and its evolution are traditionally split into two categories: the radiative mode, including ionization, heating and radiation pressure (e.g. Ciotti & Ostriker 2007), and the mechanical mode via nuclear winds and jets (e.g. Ciotti, Ostriker & Proga 2009; Shin, Ostriker & Ciotti 2010), although the physics of these feedback processes is still uncertain (see Begelman 2004, for a review). AGN feedback in many different forms has been highlighted as a possible mechanism to explain the shape of the galaxy luminosity function (e.g. Croton et al. 2006), the temperature–luminosity relationship of galaxy clusters (e.g. Bower et al. 2001), the cooling flow problem of galaxy clusters (e.g. Fabian 1994; Vernaleo & Reynolds 2006), the colour bimodality of galaxies (e.g. Smolčić 2009) and other observational phenomena. The form of AGN feedback varies among different models, but the main idea of this AGN feedback is to regulate the supply of potentially star-forming cold gas by supplying extra energy to the interstellar and intergalactic medium.

The effects of AGN on star formation can be examined in several different stages of galaxy evolution. One way is to understand the stellar populations of AGN host galaxies (see Canalizo et al. 2006, for a review). For example, the host galaxies of low-redshift narrow-line quasars have a significant fraction of recently formed (< 1 Gyr) stars (Kauffmann et al. 2003b; Liu et al. 2009). Vanden Berk et al. (2006) found similar results for broad-line quasars. The mass of molecular gas varies in AGN host galaxies, and is also an indirect measurement of their star formation potential (e.g. Papadopoulos et al. 2008; Evans et al. 2009; Wang et al. 2010). Another way is to investigate galaxies such as ultraluminous infrared galaxies (ULIRGs), hosting both AGNs and intensive star formation simultaneously (see Sanders & Mirabel 1996, for a review). Several radio-loud star-forming AGNs also show a connection

⋆E-mail: msshin@umich.edu (M-SS), strauss@astro.princeton.edu (MAS), rita.tojeiro@port.ac.uk (RT)

between the suppression of star formation and the strength of radio jets (e.g. Nesvadba et al. 2008).

As a special and rare stage in galaxy evolution, post-starburst galaxies, also known as K+A or E+A galaxies because of the characteristic features in their spectra, have recently undergone an abrupt cessation of active star formation. These galaxies do not show signs of current active star formation in the form of optical emission lines, but their stellar populations are composed both of recently formed stars (represented by A-type stars with their strong Balmer absorption lines) and of old populations (e.g. Dressler & Gunn 1983; Zabludoff et al. 1996; Quintero et al. 2004). Post-starburst galaxies are located in similar large-scale environments as are normal star-forming and quiet galaxies (Blake et al. 2004; Hogg et al. 2006), even though many post-starburst galaxies show dynamical interactions with neighbours (Yagi, Goto & Hattori 2006). Field E+A galaxies are quite heterogeneous in terms of their surface brightness distribution, velocity dispersion and luminosity despite their similar spectroscopic features (Tran et al. 2004).

There are several models to explain what causes the intensive star formation and is abrupt truncation in post-starburst galaxies. External effects on galaxies such as ram-pressure stripping might play an important role in quickly ceasing star formation (Gunn & Gott 1972; Dressler 1984). Galaxy mergers are also thought to trigger intensive star formation, and to stop it quickly without requiring feedback from a central supermassive black hole (Bekki et al. 2005) on time-scales from a few hundred Myr to few Gyr (see Falkenberg, Kotulla & Fritze 2009a, for time-scales and star formation models). Alternatively, the truncation of star formation might be caused by internal processes such as AGN feedback effects, although we do not know yet what types of AGN feedback effects are most important (Ciotti & Ostriker 2007; Ciotti et al. 2009; Ciotti, Ostriker & Proga 2010; Shin, Ostriker & Ciotti 2010). More general scenarios can be constructed by combining the internal and external processes described above (e.g. Springel, Di Matteo & Hernquist 2005; Sijacki et al. 2007; Khalatyan et al. 2008).

If the sudden cessation of star formation in post-starburst galaxies is related to AGN activity, we might expect to see several different forms of AGN activity in these objects. X-ray emission due to AGN has been reported in some post-starburst galaxies (Dewangan et al. 2000; Georgakakis et al. 2008; Brown et al. 2009). Some post-starburst galaxies also show AGN emission lines in the optical in addition to strong Balmer absorption lines (Brotherton et al. 1999; Goto 2006; Yan et al. 2006; Yang et al. 2006). Radio continuum emission thought be due to radio-mode AGN activity is also detected in some post-starburst galaxies (e.g. Liu et al. 2007). Outflows have been measured via Mg II absorbers in some luminous post-starburst galaxies, with velocities comparable to those due to AGN or extreme starbursts (Tremonti, Moustakas & Diamond-Stanic 2007).

The effects of radio AGN on star formation have not been investigated fully in post-starburst galaxies. The expected lifetime of radio emission is between 1.5×10^7 and 10^8 yr (Alexander & Leahy 1987; Blundell & Rawlings 2000; Bird, Martini & Kaiser 2008; Shabala et al. 2008), much shorter than the ages of A-type stars, $\sim$1 Gyr, found in post-starburst galaxies. If there is a close link between launching radio-mode AGN activity and quenching star formation quickly in the transition to the post-starburst phase, radio-emitting AGN activity in post-starburst galaxies should therefore be rare.

In this paper, we focus on radio-mode AGN feedback and its connection to quenching star formation by studying the radio properties of Sloan Digital Sky Survey (SDSS; York et al. 2000) post-starburst galaxies (Goto 2007). To this end, we investigate what kind of post-starburst galaxies show radio emission from AGN activity. Based on stellar population fits to the SDSS spectra, we also examine how the quantity of recent star formation is related to the strength of the radio-mode AGN activity. Connections between stellar populations and radio emission will give us insights about triggering mechanisms of recent starbursts and AGN activity.

The paper is organized as follows. In Section 2, we introduce our sample of post-starburst galaxies, and explain how we identify radio sources among post-starburst galaxies. Analysis of the stellar populations in our sample galaxies is given in Section 3. We present the radio properties of our sample, as well as the constraints on mechanical feedback, in Section 4. Discussion and conclusions are given in Section 5. Throughout the paper, we use $H_0 = 70\ \mathrm{km\ s^{-1}\ Mpc^{-1}}$, $\Omega_\mathrm{m} = 0.3$ and $\Omega_\Lambda = 0.7$.

2 IDENTIFICATION OF RADIO SOURCES

Our sample of post-starburst galaxies is from Goto (2007), and consists of galaxies that have a continuum dominated by A-type stars, but are optically completely quiet in both star formation and AGN activity, as measured by the absence of both the [O II]λ3727 and Hα emission lines. The sample of post-starburst galaxies includes all objects which do not have detectable [O II]λ3727 and Hα emission lines in their SDSS spectra from the SDSS Data Release 5 (Adelman-McCarthy et al. 2007), but show a rest-frame Hδ equivalent width (EW) in absorption of >5 Å (see Falkenberg et al. 2009a; Oemler et al. 2009; Poggianti et al. 2009, for various different criteria for defining E+A galaxies). The redshifts of the galaxies in the sample range from 0.0327 to 0.3421, where the upper limit guarantees that the Hα line is included in the SDSS spectra.

We identify radio sources by matching the post-starburst galaxy sample of 564 galaxies to the Faint Images of the Radio Sky at Twenty-centimetres (FIRST) catalogue (Becker White & Helfand 1995). The Very Large Array (VLA) FIRST Survey covers 9030 deg^2 at 1.4 GHz. 534 galaxies in our sample lie within the FIRST coverage. We drop 22 galaxies whose spectra have bad pixels affecting the results of the population synthesis modelling we describe below, leaving 513 galaxies as our main sample. 137 of these galaxies have a FIRST detection within 2 arcmin.

We visually inspect the morphology of the radio sources in the FIRST images, and evaluate the goodness of the positional match between the SDSS galaxies and the radio sources. If radio sources are positionally coincident with other SDSS objects in the field, we do not consider these as good matches. Because the angular distance between the post-starburst galaxies and other SDSS sources is generally more than 10 arcsec in these cases, we are unlikely to miss radio sources actually corresponding to the post-starburst galaxies. We find 11 unambiguous radio-emitting post-starburst galaxies, as well as one insecure match in which the radio source is not coincident with either the post-starburst galaxy or any other SDSS object, but is adjacent to the post-starburst galaxy. These sources are listed in Table 1 and Fig. 1. We conclude that the radio flux of the remaining 501 galaxies at 1.4 GHz is below the FIRST detection limit of about 1 mJy.

The flux limit of 1 mJy corresponds to a radio luminosity ranging from $10^{21.4}$ to $10^{23.7}\ \mathrm{W\ Hz^{-1}}$ for the redshifts of our sample, assuming a power-law spectral energy distribution with a spectral index between -1 and 1. Because this luminosity is larger than that of some genuine radio AGN (e.g. Best et al. 2005), there may be radio AGNs among the sources undetected in the FIRST survey.

Two galaxies in our sample, SDSSJ160808.7+394755 and SDSSJ161910.4+064223, have two resolved radio sources in the

Table 1. Radio-emitting post-starburst galaxies.

SDSS name	Redshift	$F_{\rm int}^{\rm FIRST}$[a] (mJy)	rms$^{\rm FIRST}$[b] (mJy)	$F^{\rm NVSS}$[c] (mJy)	rms$^{\rm NVSS}$[d] (mJy)
SDSSJ082254.8+192128	0.0626	0.70	0.15	–	–
SDSSJ084542.7+292932	0.1475	0.96	0.14	–	–
SDSSJ092023.1+394039	0.0690	7.96	0.13	4.0	0.4
SDSSJ094818.6+023004	0.0604	2.79	0.14	2.7	0.5
SDSSJ095842.6+631845	0.2426	22.52	1.75	21.3	0.8
SDSSJ101342.7+125135	0.1391	1.24	0.13	–	–
SDSSJ132542.3+325503	0.2926	1.71	0.12	–	–
SDSSJ154322.4+331018[e]	0.1265	3.98	0.15	5.2	0.4
SDSSJ160808.7+394755[f]	0.1909	12.93	0.14	35.8	1.5
SDSSJ161910.4+064223[f]	0.2100	45.20	0.14	77.2	3.0
SDSSJ165958.0+213640	0.1567	2.92	0.14	2.7	0.5
SDSSJ170859.2+322053[g]	0.1206	1.10	0.14	2.8	0.5

[a]The integrated flux density at 1.4 GHz is extracted from the FIRST catalogue (Becker et al. 1995).
[b]The rms noise is measured locally at the source position in the FIRST catalogue.
[c]The integrated 1.4 GHz flux density is given in the NVSS catalogue (Condon et al. 1998). A typical detection limit is about 2.5 mJy in the NVSS catalogue.
[d]The mean error of the NVSS flux density.
[e]The match is uncertain for this object.
[f]In the FIRST images, a pair of radio sources is seen around the SDSS galaxy. For these objects, we use the NVSS measurements.
[g]This galaxy has a companion galaxy (Yamauchi et al. 2008).

FIRST images, which we interpret as a pair of radio lobes. No neighbour objects around SDSSJ161910.4+064223 are matched to these sources. Projection of unrelated radio sources is one alternative explanation. But although the post-starburst galaxy does not lie right on the line connecting the two resolved radio sources, the redshift of the galaxy and the size of radio lobes support our inference that the host system of the lobes is the post-starburst galaxy.

The positional match is less certain in the case of SDSSJ154322.4+331018. The bright extended radio source is offset from the galaxy by about 10 arcsec, and has no other optical counterpart that is positionally coincident. We assume that the radio source is physically associated with the post-starburst galaxy, but cannot prove it without further investigation of deep high-resolution radio imaging or deep optical imaging to find possible faint optical counterparts. Therefore, we tag this object as an uncertain match.

We also matched our sample against the NRAO VLA Sky Survey (NVSS) catalogue (Condon et al. 1998). The NVSS catalogue has a flux limit of 2.5 mJy, but does a better job of measuring the integrated flux of extended radio sources (see Ivezić et al. 2002, for a discussion on matching SDSS objects to the FIRST and NVSS catalogues). Table 1 compares the flux measurements between the FIRST and NVSS catalogue. There are serious discrepancies in the flux levels for the two double sources; the flux from the FIRST catalogue is for only one of the radio lobes in SDSSJ160808.7+394755 and SDSSJ161910.4+064223. When adding the fluxes from the two lobes, the total flux from the FIRST catalogue is comparable to the NVSS fluxes. Therefore, we use the flux from the NVSS catalogue for these two objects.

3 POPULATION SYNTHESIS MODEL

We use the Versatile Spectral Analysis (VESPA) method (Tojeiro et al. 2007, 2009) to determine stellar masses, star formation histories and stellar metallicity distributions for all 513 galaxies in our sample. The VESPA method models the SDSS spectra as the linear combination of stellar populations in up to 16 age bins; the metallicity of the stars formed in each bin can have one of five metallicities. The number of age bins in population modelling depends on the amount of extractable information in the spectra given their signal-to-noise ratios. The model also includes one dust extinction for young stellar populations with age <0.3 Gyr, and another dust extinction factor for old stellar populations.

The derived star formation and metallicity histories are limited by the 3 arcsec spatial coverage of the spectrograph fibres. To correct for this fibre effect, we assume that the derived star formation and metallicity history from the SDSS fibre spectrum are appropriate for the entire galaxy. Thus we scale the spectrum by the difference between the SDSS fibre magnitude and the Petrosian magnitude in r band. The average ratio of the fibre flux to the Petrosian flux is about 11 per cent for the objects in our sample. Because we focus on the effects of radio-mode AGN activity which should take place at the galaxy centre, this fibre effect is not a serious issue in estimating the mass fraction of recently formed stars.

Fig. 2 presents the derived star formation and metallicity history for two galaxies in our sample. SDSSJ094818.6+023004, which shows unambiguous radio emission in the FIRST data (Fig. 1), has Hδ EW 6.18 ± 1.02 Å, and most of its stellar mass is younger than 1 Gyr. Meanwhile, SDSSJ160417.3+155503, which does not have a FIRST counterpart, is intermediate between a strong post-starburst galaxy and a passively evolving galaxy, with EW(Hδ) $= 5.46 \pm 1.25$ Å. Its dominant stellar population is also older than 1 Gyr.

The derived stellar masses of the galaxies in the sample range from about $10^{8.4}$ to $10^{11.7}\,{\rm M}_{\odot}$, as presented in Fig. 3. The typical statistical uncertainty of the stellar mass is about 40 per cent for objects in our sample, although systematic effects such as uncertainties in the initial mass function and the stellar population models used can affect the derived stellar mass (Tojeiro et al. 2009). Table 2 lists the stellar masses of the 12 galaxies with radio detections.

An interesting quantity is the fraction of stellar mass that is recently formed in our sample of post-starburst galaxies.

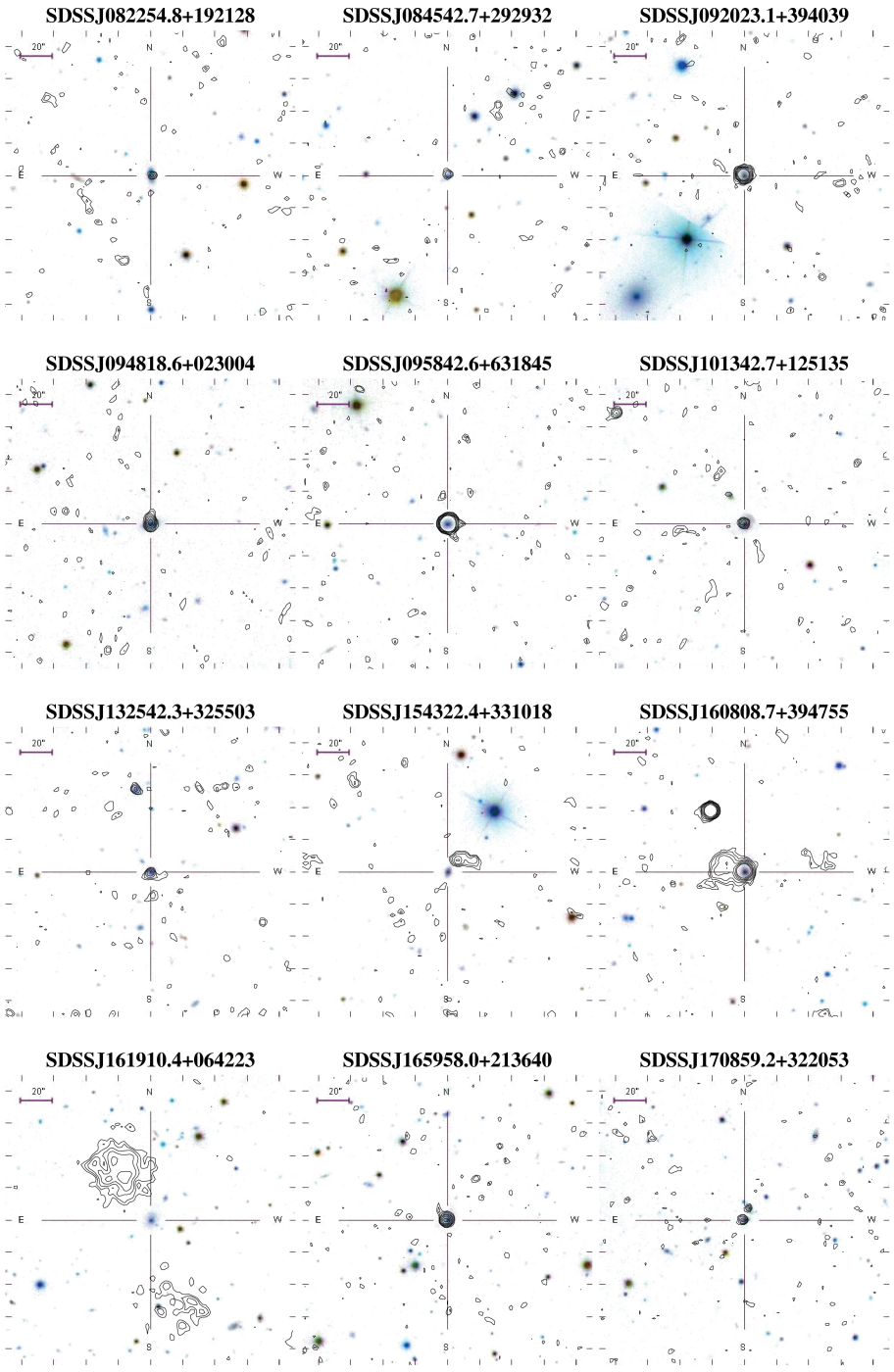

Figure 1. Radio-emitting post-starburst galaxies. Except for SDSSJ154322.4+331018, all galaxies are well matched to the coordinates of radio sources. SDSSJ160808.7+394755 and SDSSJ161910.4+064223 are suspected to have double radio lobes. Colour images are the SDSS *gri* cutout images of size 3× 3 arcmin^2, while the contour lines are from the FIRST images.

The fraction has a very broad distribution (see Fig. 3), implying that a wide range of star formation and metallicity histories can give rise to the spectroscopic features of post-starburst galaxies (e.g. Balogh et al. 1999; Kauffmann et al. 2003a; Martin et al. 2007; Falkenberg et al. 2009a; Falkenberg, Kotulla & Fritze 2009b).

Fig. 4 shows that the mass fraction of young stars in galaxies is only weakly related to the strong Hδ absorption line which was used to compile the sample of post-starburst galaxies. We used both 635 Myr and 1 Gyr as the possible upper age limit to define the young stellar population, but we did not find a strong correlation between the young mass fraction and the strength of the Hδ absorption line in either case. Because various star formation histories can produce a given Hδ absorption line strength by varying the strength of recent starbursts and their time-scales (e.g. Falkenberg et al. 2009a), it is not surprising that we found no strong correlation.

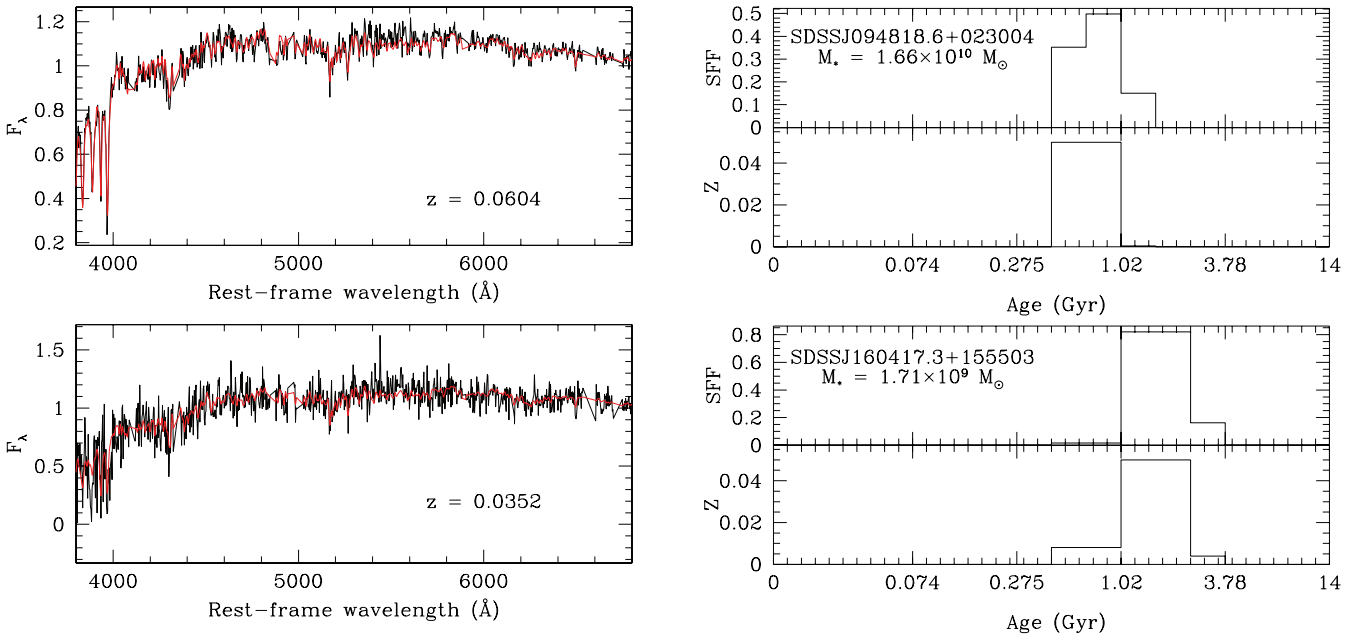

Figure 2. Examples of star formation and metallicity histories with the SDSS spectra. SDSSJ094818.6+023004 (top) is a radio source, and is more massive than SDSSJ160417.3+155503, a radio-quiet source (bottom). The reconstructed spectra by the VESPA method are represented as red lines in the left-hand panel. The star formation histories (star formation fraction) and metallicity distributions (Z) derived by the VESPA method (right-hand panel) show that the young stellar population is metal rich in both spectra.

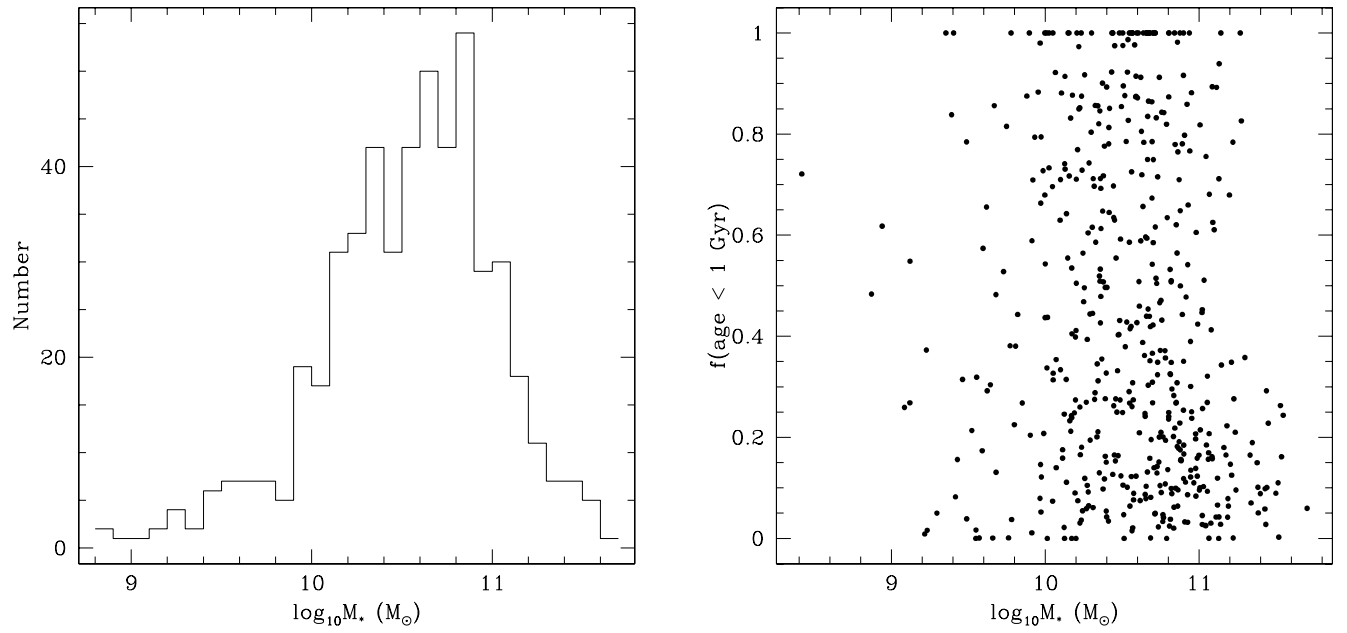

Figure 3. Distribution of total stellar mass for the post-starburst galaxies in our sample (left-hand panel). The mass fraction of the stellar population younger than 1 Gyr (right-hand panel) shows a broad distribution, and no correlation with stellar mass.

4 RADIO PROPERTIES

4.1 Radio emission

Radio emission in a galaxy can be due to either AGN or star formation. Even though none of our sample galaxies shows any strong star formation signature in their optical spectra (by definition), it is possible that the galaxies are heavily dust extincted (Shioya & Bekki 2000), or that weak residual star formation activity exists associated with the detected radio emission, which is not strong enough to produce optical emission lines. The time-scale of radio emission from star formation can range from about 10^7 to 10^8 yr, depending on the supply and escape of cosmic rays and their environment as well as the lifetime of H II regions (Chi & Wolfendale 1990; Helou & Bicay 1993). This time-scale might be long enough to be an explanation for at least some post-starburst galaxies. Therefore, it is necessary to examine whether the radio emission is due to star formation.

AGN radio emission can be distinguished in two ways (see Mushotzky 2004, for a review). First, multiple radio emission

Table 2. Radio luminosities and stellar masses of the identified radio sources.

SDSS name	$\log_{10}L_{1.4\ \mathrm{GHz}}^{\alpha=-1}$ ($\mathrm{WHz^{-1}}$)	$\log_{10}L_{1.4\ \mathrm{GHz}}^{\alpha=0}$ ($\mathrm{WHz^{-1}}$)	$\log_{10}L_{1.4\ \mathrm{GHz}}^{\alpha=1}$ ($\mathrm{WHz^{-1}}$)	M_* ($10^{10}\,\mathrm{M_\odot}$)
SDSSJ082254.8+192128	21.82	21.85	21.87	1.81
SDSSJ084542.7+292932	22.75	22.81	22.87	2.88
SDSSJ092023.1+394039	22.96	22.99	23.02	4.40
SDSSJ094818.6+023004	22.39	22.41	22.44	1.66
SDSSJ095842.6+631845	24.60	24.70	24.79	8.35
SDSSJ101342.7+125135	22.81	22.86	22.92	4.94
SDSSJ132542.3+325503	23.67	23.78	23.89	7.91
SDSSJ154322.4+331018	23.22	23.28	23.33	2.20
SDSSJ160808.7+394755	24.57	24.65	24.72	5.59
SDSSJ161910.4+064223	25.00	25.08	25.16	9.54
SDSSJ165958.0+213640	23.29	23.35	23.42	2.22
SDSSJ170859.2+322053	22.62	22.67	22.72	4.88

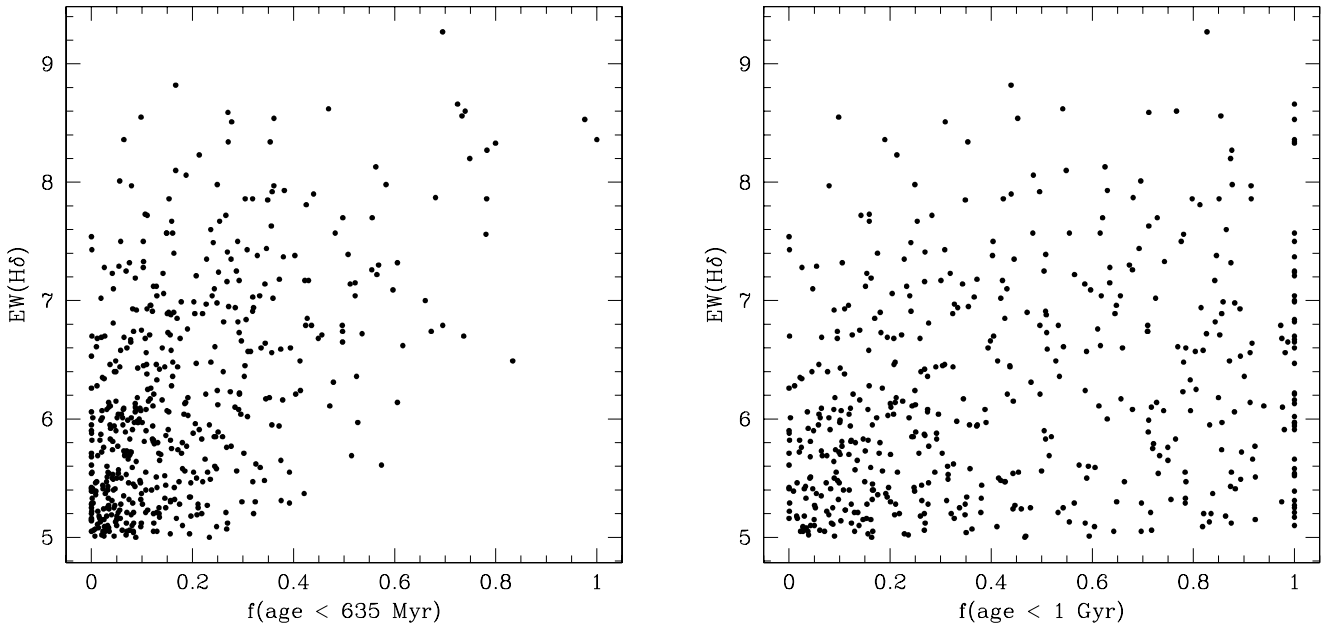

Figure 4. Rest-frame EW of the Hδ absorption line from Goto (2007) with respect to the recent star formation fraction. The EW is weakly correlated with the fraction of stellar mass younger than 635 Myr (left-hand panel). But we do not find a correlation with the fraction of stellar mass younger than 1 Gyr (right-hand panel) (e.g. Kauffmann et al. 2003a; Martin et al. 2007; Falkenberg et al. 2009a). The typical error of EW(Hδ) is about 1 Å.

components such as lobes or jets are signatures of AGN activity (Fanaroff & Riley 1974; Reviglio & Helfand 2006). In our sample, we find extended multiple emission regions that are not matched to the optical light distribution in SDSSJ094818.6+023004, SDSSJ16080808.7+394755 and SDSSJ161910.4+064223 as well as the uncertain case SDSSJ154322.4+331018 (see Fig. 1). Secondly, the radio luminosities of these galaxies can be used to identify radio-emitting AGNs. The radio-to-optical flux ratio or radio luminosity itself can be used statistically to recognize radio emission from AGN activity (e.g. Ivezić et al. 2002; Best et al. 2005). But with the small number of objects in our sample, it is not safe to use the radio-to-optical flux ratio to distinguish radio emission from AGN and from star formation. Moreover, the boundary of the flux ratio between the two emission sources is not sharp (e.g. Reviglio & Helfand 2006).

If we assume that the radio emission is due entirely to ongoing star formation (e.g. Goto 2004), we can convert the observed radio luminosity to the expected current star formation rate (SFR) following the conversion given by Yun et al. (2001):

$$\mathrm{SFR}\ (\mathrm{M_\odot\ yr^{-1}}) \ = \ 5.9 \times 10^{-22}\ L_{1.4\ \mathrm{GHz}}\ (\mathrm{W\,Hz^{-1}})$$

assuming the Salpeter initial mass function (Salpeter 1955) with a mass range from 0.1 to 100 $\mathrm{M_\odot}$ (see Bell 2003; Hopkins et al. 2003, for different conversions). The coefficient in this equation has a statistical scatter of about 30 per cent (Yun et al. 2001). When we adopt the Chabrier (Chabrier 2003) initial mass function, the difference in the estimated SFRs with these two initial mass functions is $\log_{10}\mathrm{SFR_{Salpeter}} - \log_{10}\mathrm{SFR_{Chabrier}} \sim 0.186$ (Bardelli et al. 2009). For our 12 radio post-starburst galaxies, radio luminosities are estimated for three different spectral indices ($\alpha = -1, 0, 1$)[1] (Tongue & Westpfahl 1995) for a power-law energy distribution $F_\nu \propto \nu^\alpha$. The radio luminosity $L_{1.4\ \mathrm{GHz}}$ ranges from about $10^{21.8}$ to $10^{25.2}\ \mathrm{W\,Hz^{-1}}$,

[1] $\alpha = -0.5$ is the conventional border between steep and flat-spectrum sources.

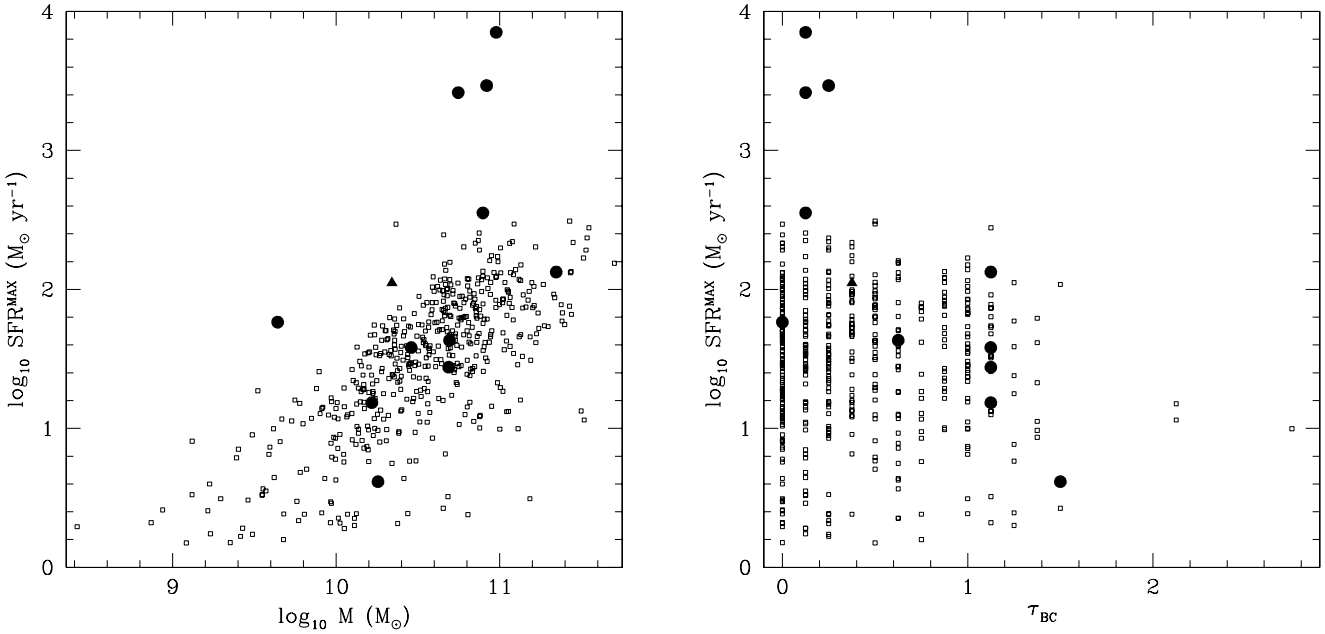

Figure 5. Upper limit of the SFR derived from the observed radio emission (assuming a radio spectral index $\alpha = 0$) as a function of mass (left-hand panel) and dust-extinction optical depth of the young stellar population ($\tau_{\rm BC}$) from the VESPA method (right-hand panel). For galaxies not matched to radio objects (empty squares), we plot the 2σ upper limit of radio luminosity corresponding to 1 mJy flux density at 1.4 GHz. Except for the uncertain match SDSSJ154322.4+331018 (triangle), objects with matched radio sources are shown as circles.

as presented in Table 2. For the galaxies which have no detectable radio counterparts, we use the radio flux upper limit of 1 mJy at 1.4 GHz.

Fig. 5 shows the resulting predicted SFRs as a function of stellar mass. All galaxies with detected radio emission except SDSSJ082254.8+192128 would have SFR $> 10\,{\rm M}_\odot\ {\rm yr}^{-1}$ assuming that the radio emission is due entirely to ongoing star formation. This level of hidden star formation seems highly unlikely given the absence of strong emission lines such as [O II] and Hα, as we now show.

We estimate the expected unextincted luminosity and EW of the [O II]λ3727 emission line from the SFR upper limit derived earlier, assuming that the radio emission is from current star formation. Using the conversion from SFR to [O II] luminosity from Hopkins et al. (2003), we derive the expected EW,

$$\mathrm{EW_{line}} \sim \frac{L_{[\mathrm{O\,II}]}}{P_c([\mathrm{O\,II}])} = \frac{\mathrm{SFR\ (M_\odot\ yr^{-1})}\ 2.97\times10^{33}\ \mathrm{(W)}}{P_c([\mathrm{O\,II}])},$$

where P_c is the continuum at 3727 Å. For SDSSJ082254.8+192128, which has the lowest expected SFR $\sim 4\,{\rm M}_\odot\ {\rm yr}^{-1}$ among the radio sources, we find an EW of about 260 Å, which is much larger than the observational limit of EW([O II]) = 0.63 Å (Goto 2007). This constraint on the EW is not affected by dust extinction, which affects continuum and line emission equally. It is a reasonable assumption that both emission lines and the blue stellar continuum originate from the same stellar population in the case of the highly obscured intensive star-forming galaxies which we consider here. It is unlikely that selective high dust extinction of the emission-line flux can explain the absence of emission lines with this large expected EW.

We also examine the optical depth for dust extinction ($\tau_{\rm BC}$) which is applied to the young stellar population in the VESPA analysis (Tojeiro et al. 2007). Although $\tau_{\rm BC}$ might be less reliable than the constraint with EW $_{\rm line}$, the distribution of $\tau_{\rm BC}$ should be at least consistent with the constraint from the expected EW. Fig. 5 shows that $\tau_{\rm BC}$ is low for sources of high radio luminosity. This trend is opposite to what would be needed to explain the absence of [O II] emission if the radio emission is due to star formation. We thus conclude that the radio emission in these 12 galaxies is dominated by AGN activity.

4.2 Feedback energy and recent star formation

Radio luminosity has been commonly used as a tracer of mechanical energy input by radio-mode AGN feedback. A simple scaling relation, albeit with non-negligible scatter, between radio luminosity and mechanical power has been suggested (e.g. Bîrzan et al. 2004). Adopting the scaling relationship from Bîrzan et al. (2008),

$$\log_{10}\left(\frac{L_{\rm mech}}{10^{42}\ {\rm erg\ s^{-1}}}\right) = 0.35\log_{10}\left(\frac{L_{1.4\ {\rm GHz}}}{10^{24}\ {\rm W\ Hz^{-1}}}\right) + 1.85,$$

we estimate the mechanical power $L_{\rm mech}$ from radio-mode AGN activity from the measured $L_{1.4\ {\rm GHz}}$ for the 12 objects which are matched to radio sources.

The mechanical power in radio-emitting samples ranges from 1.2×10^{43} to $1.8\times10^{44}\ {\rm erg\,s^{-1}}$, as shown in Fig. 6. Interestingly, the mechanical energy is higher for objects of higher galaxy stellar mass, in agreement with Best et al. (2005), who show that luminous radio sources are more likely to be hosted by more massive galaxies. Although our sample is radio flux limited, the absence of luminous radio sources for low-mass galaxies is not due to selection effects, as the distribution of the radio luminosity upper limits for objects without radio counterparts shows in Fig. 5. This trend is not surprising because massive galaxies host massive central black holes, which can produce radio jets with a large amount of mechanical power (see Bender et al. 1989; Meier 2003; Best et al. 2005; Kormendy et al. 2009; Bardelli et al. 2010, for a discussion). It also suggests that the mechanical power is correlated with the old stellar population, which dominates the stellar mass.

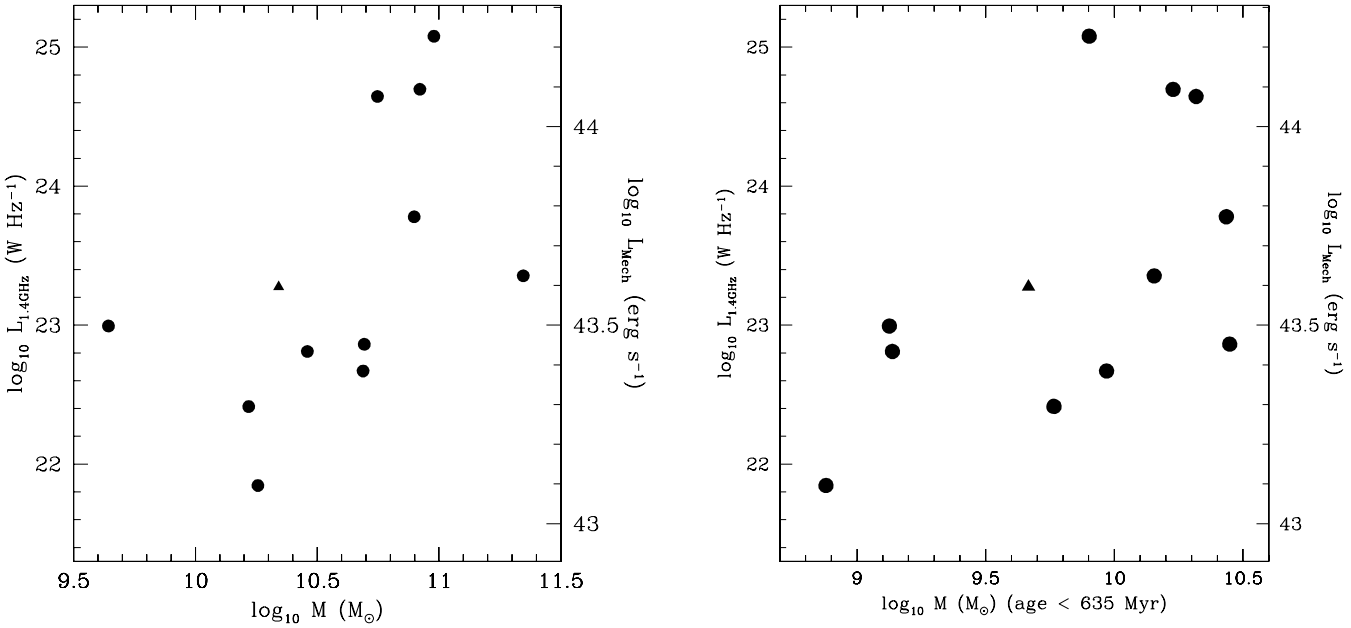

Figure 6. Correlations between radio luminosity (i.e. mechanical power) and stellar mass (left-hand panel), and the mass of the stellar population younger than 635 Myr (right-hand panel). Symbols are same as in Fig. 5. Among the 12 radio-detected objects, only SDSSJ101342.7+125135 has more than 50 per cent of its stellar mass younger than 635 Myr; it has a total stellar mass of $4.9 \times 10^{10}\,M_{\odot}$.

In contrast, no correlation of recently formed stellar mass with mechanical power output is apparent, as presented in Fig. 6. In elliptical galaxies with hot gas haloes, Allen et al. (2006) found a tight positive correlation between Bondi accretion power and jet power. Because the SFR also shows a strong correlation with the black hole growth rate at the centre of cooling flows (Rafferty et al. 2006), a correlation between jet power and recently formed stellar mass is expected in galaxies with significant cooling flows. But our sample is not consistent with this picture. This result suggests that the recent star formation was ignited by a cooling flow in only a fraction at best of radio post-starburst galaxies in our sample.

5 DISCUSSION AND CONCLUSIONS

We find that the abrupt cessation of star formation in post-starburst galaxies is not caused solely by radio-mode feedback from AGN. The typical lifetime of radio emission is of the order of 10^7–10^8 yr (Blundell & Rawlings 2000; Bird et al. 2008; Shabala et al. 2008). However, the post-starburst phase can last up to ∼1 Gyr (the lifetime of A-type stars), and must be longer than ∼1 Myr which is constrained by the typical lifetime of massive stars that produce ionizing photons and emission lines (Charlot & Fall 2000). Therefore, the existence of radio-emitting post-starburst galaxies implies that radio-mode AGN activity, which is the source of the radio emission we observe, should form after the end of the recent starburst.

But we cannot rule out that the rest of the objects in our sample (i.e. those without detectable radio emission) might have experienced radio-mode feedback and the cessation of star formation concurrently. Because our sample is flux limited in the radio, we were unable to prove that the late stage of post-starburst galaxies always accompanies radio-mode AGN activity after the end of star formation, particularly for massive post-starburst galaxies. Future deep radio surveys of post-starburst galaxies will be required to detect low-luminosity radio emission in the rest of our sample galaxies.

This time delay between the cessation of star formation and radio-emitting AGN activity was already suggested for some radio-excess *IRAS* galaxies based on the same kind of time-constraint arguments as we have given (Buchanan et al. 2006). This kind of time delay is also found in the nuclei of local Seyfert galaxies based on ages of stellar populations (Davies et al. 2007). Although radio excess in *IRAS* and Seyfert galaxies might evolve differently than radio emission in post-starburst galaxies, the delay between fuelling the central black hole and recent star formation is about 50 to a few hundred Myr (e.g. Schawinski et al. 2007). In our constraint, the upper limit of this time delay can be up to about 1 Gyr, which is basically limited by the age of post-starburst stellar population. The physics of this time delay is still uncertain, although observational constraints suggest that strong fuelling on to a central supermassive black hole occurs after intensive star formation, and is regulated by the recent and ongoing star formation in a galaxy (see Shlosman, Begelman & Frank 1990; Davies et al. 2007, for a discussion of the time delay).

In the *cooling flow paradigm* of early-type galaxies, cold gas in the cooling flow forms new stars and also fuels the central black hole. If so (Cardiel, Gorgas & Aragon-Salamanca 1998; Bildfell et al. 2008; O'Dea et al. 2008; Pipino et al. 2009), the spectral energy distribution might go through a post-starburst phase, with AGN feedback (e.g. Ciotti et al. 2010). Radio-emitting post-starburst galaxies without evidence for galaxy interactions might have been fed by a cooling flow.

Alternatively, let us consider the galaxy interaction scenario. Many post-starburst galaxies are thought to be merger remnants, where the termination of star formation seems to occur before the radio-mode AGN activity (e.g. Tadhunter et al. 2005; Emonts et al. 2006). Moreover, powerful radio galaxies seem to be more commonly hosted by galaxy mergers than are less luminous radio galaxies and radio-quiet ellipticals (Heckman et al. 1986; Wilson & Colbert 1995). One of our sources, SDSSJ170859.2+322053, is already known to be a merging/interacting galaxy (Yamauchi, Yagi &

Goto 2008), but follow-up deep optical imaging of the other radio-emitting post-starburst galaxies in our sample may reveal mergers, allowing an investigation of a link between galaxy interaction, star formation triggering, star formation quenching and the initiation of radio-mode AGN activity. Numerical simulations of galaxy mergers or interactions including radio-mode AGN activity would allow a test of the observed features of morphologically disturbed radio-emitting post-starburst galaxies (e.g. Sijacki et al. 2007).

The key difference between the two scenarios might be different time delays between the end of intensive star formation and the ignition of AGN activity (e.g. Wills et al. 2008). Further investigation of distinctive spectroscopic features from different time delays and star formation histories may yield the evidence of these two processes in the post-starburst phase (e.g. Falkenberg et al. 2009a).

In this paper, we did not consider that possible early radio AGN activity, which does not correspond to what we detect now in radio, might be an effective way to quench star formation. For example, the radio galaxy 3C 236 has both multiple stellar populations and multiple radio sources which might have formed concurrently in several episodes (Tremblay et al. 2010). But because the visible radio relics of the past active phase dim fast and appears at low frequencies within 1 Gyr, it might be difficult to detect activity older than about 10^8 yr in radio data (Kaiser & Cotter 2002; Godambe et al. 2009). Deep X-ray imaging of radio-emitting post-starburst galaxies might be helpful to discover the fossil record of the past radio-mode AGN activity (Juett et al. 2008).

In addition to the delayed radio-mode AGN activity discussed in this paper, there might be other kinds of AGN feedback effects which can cause the sudden cessation of star formation in post-starburst galaxies. For instance, it is already known that some post-starburst galaxies show clear spectroscopic features of quasar emission, implying that quasar activity lasts longer than star formation or is triggered after the peak of star formation (e.g. Brotherton et al. 1999). X-ray emission from AGN accretion is also found in some post-starburst galaxies (e.g. Brown et al. 2009). It will be important to understand what kinds of post-starburst galaxies do not have any kinds of AGN feedback effects, and how the types of AGN activity are related to other properties of post-starburst galaxies such as merger stages and environment.

ACKNOWLEDGMENTS

We are grateful to Jeremiah Ostriker, James Gunn, Gillian Knapp, Renyue Cen and Christy Tremonti for useful discussions and careful reading of the manuscript. We would like to thank Eric Pellegrini and Ryan Porter for useful discussions. We thank the anonymous referee for comments which improved this manuscript. M-SS was supported by the Charlotte Elizabeth Procter Fellowship of Princeton University. M-SS and MAS acknowledge the support of NSF grant AST-0707266.

Funding for the SDSS and SDSS-II has been provided by the Alfred P. Sloan Foundation, the Participating Institutions, the National Science Foundation, the US Department of Energy, the National Aeronautics and Space Administration, the Japanese Monbukagakusho, the Max Planck Society and the Higher Education Funding Council for England. The SDSS web site is http://www.sdss.org/. The SDSS is managed by the Astrophysical Research Consortium for the Participating Institutions. The Participating Institutions are the American Museum of Natural History, Astrophysical Institute Potsdam, University of Basel, University of Cambridge, Case Western Reserve University, University of Chicago, Drexel University, Fermilab, the Institute for Advanced Study, the Japan Participation Group, Johns Hopkins University, the Joint Institute for Nuclear Astrophysics, the Kavli Institute for Particle Astrophysics and Cosmology, the Korean Scientist Group, the Chinese Academy of Sciences (LAMOST), Los Alamos National Laboratory, the Max-Planck-Institute for Astronomy (MPIA), the Max-Planck-Institute for Astrophysics (MPA), New Mexico State University, Ohio State University, University of Pittsburgh, University of Portsmouth, Princeton University, the United States Naval Observatory and the University of Washington.

REFERENCES

Adelman-McCarthy J. K. et al., 2007, ApJS, 172, 634
Alexander P., Leahy J. P., 1987, MNRAS, 225, 1
Allen S. W., Dunn R. J. H., Fabian A. C., Taylor G. B., Reynolds C. S., 2006, MNRAS, 372, 21
Balogh M. L., Morris S. L., Yee H. K. C., Carlberg R. G., Ellingson E., 1999, ApJ, 527, 54
Bardelli S. et al., 2009, A&A, 495, 431
Bardelli S. et al., 2010, A&A, 511, A1
Becker R. H., White R. L., Helfand D. J., 1995, ApJ, 450, 559
Begelman M. C., 2004, inL. C. Ho, ed., Coevolution of Black Holes and Galaxies. Cambridge Univ. Press, Cambridge, p. 374
Bekki K., Couch W. J., Shioya Y., Vazdekis A., 2005, MNRAS, 359, 949
Bell E. F., 2003, ApJ, 586, 794
Bender R., Surma P., Doberetner S., Moellenhoff C., Madejsky R., 1989, A&A, 217, 35
Best P. N., Kauffmann G., Heckman T. M., Brinchmann J., Charlot S., Ivezić Ž., White S. D. M., 2005, MNRAS, 362, 25
Bildfell C., Hoekstra H., Babul A., Mahdavi A., 2008, MNRAS, 389, 1637
Bird J., Martini P., Kaiser C., 2008, ApJ, 676, 147
Bîrzan L., Rafferty D. A., McNamara B. R., Wise M. W., Nulsen P. E. J., 2004, ApJ, 607, 800
Bîrzan L., McNamara B. R., Nulsen P. E. J., Carilli C. L., Wise M. W., 2008, ApJ, 686, 859
Blake C. et al., 2004, MNRAS, 355, 713
Bland-Hawthorn J., Veilleux S., Cecil G., 2007, Ap&SS, 311, 87
Blundell K. M., Rawlings S., 2000, AJ, 119, 1111
Bower R. G., Benson A. J., Lacey C. G., Baugh C. M., Cole S., Frenk C. S., 2001, MNRAS, 325, 497
Brotherton M. S. et al., 1999, ApJ, 520, L87
Brown M. J. I. et al., 2009, ApJ, 703, 150
Buchanan C. L., McGregor P. J., Bicknell G. V., Dopita M. A., 2006, AJ, 132, 27
Canalizo G., Stockton A., Brotherton M. S., Lacy M., 2006, New Astron. Rev., 50, 650
Cardiel N., Gorgas J., Aragon-Salamanca A., 1998, MNRAS, 298, 977
Chabrier G., 2003, PASP, 115, 763
Charlot S., Fall S. M., 2000, ApJ, 539, 718
Chi X., Wolfendale A. W., 1990, MNRAS, 245, 101
Cid Fernandes R., Heckman T., Schmitt H., González Delgado R. M., Storchi-Bergmann T., 2001, ApJ, 558, 81
Ciotti L., Ostriker J. P., 2007, ApJ, 665, 1038
Ciotti L., Ostriker J. P., Proga D., 2009, ApJ, 699, 89
Ciotti L., Ostriker J. P., Proga D., 2010, ApJ, 717, 708
Condon J. J., Cotton W. D., Greisen E. W., Yin Q. F., Perley R. A., Taylor G. B., Broderick J. J., 1998, AJ, 115, 1693
Croton D. J. et al., 2006, MNRAS, 365, 11
Davies R. I., Sánchez F. M., Genzel R., Tacconi L. J., Hicks E. K. S., Friedrich S., Sternberg A., 2007, ApJ, 671, 1388
Dewangan G. C., Singh K. P., Mayya Y. D., Anupama G. C., 2000, MNRAS, 318, 309
Dressler A., 1984, ARA&A, 22, 185
Dressler A., Gunn J. E., 1983, ApJ, 270, 7
Emonts B. H. C., Morganti R., Tadhunter C. N., Holt J., Oosterloo T. A., van der Hulst J. M., Wills K. A., 2006, A&A, 454, 125
Evans A. S. et al., 2009, AJ, 138, 262

Fabian A. C., 1994, ARA&A, 32, 277
Falkenberg M. A., Kotulla R., Fritze U., 2009a, MNRAS, 397, 1940
Falkenberg M. A., Kotulla R., Fritze U., 2009b, MNRAS, 397, 1954
Fanaroff B. L., Riley J. M., 1974, MNRAS, 167, 31
Farrah D., Afonso J., Efstathiou A., Rowan-Robinson M., Fox M., Clements D., 2003, MNRAS, 343, 585
Georgakakis A. et al., 2008, MNRAS, 385, 2049
Godambe S., Konar C., Saikia D. J., Wiita P. J., 2009, MNRAS, 396, 860
Goto T., 2004, A&A, 427, 125
Goto T., 2006, MNRAS, 369, 1765
Goto T., 2007, MNRAS, 381, 187
Gunn J. E., Gott J. R., III, 1972, ApJ, 176, 1
Heckman T. M., Smith E. P., Baum S. A., van Breugel W. J. M., Miley G. K., Illingworth G. D., Bothun G. D., Balick B., 1986, ApJ, 311, 526
Helou G., Bicay M. D., 1993, ApJ, 415, 93
Hogg D. W., Masjedi M., Berlind A. A., Blanton M. R., Quintero A. D., Brinkmann J., 2006, ApJ, 650, 763
Hopkins A. M. et al., 2003, ApJ, 599, 971
Ivezić Ž. et al., 2002, AJ, 124, 2364
Juett A. M. et al., 2008, ApJ, 672, 138
Kaiser C. R., Cotter G., 2002, MNRAS, 336, 649
Kauffmann G. et al., 2003a, MNRAS, 341, 33
Kauffmann G. et al., 2003b, MNRAS, 346, 1055
Khalatyan A., Cattaneo A., Schramm M., Gottlöber S., Steinmetz M., Wisotzki L., 2008, MNRAS, 387, 13
Kormendy J., Fisher D. B., Cornell M. E., Bender R., 2009, ApJS, 182, 216
Liu C. T., Hooper E. J., O'Neil K., Thompson D., Wolf M., Lisker T., 2007, ApJ, 658, 249
Liu X., Zakamska N. L., Greene J. E., Strauss M. A., Krolik J. H., Heckman T. M., 2009, ApJ, 702, 1098
Lonsdale C. J., Farrah D., Smith H. E., 2006, Astrophys. Update, 2, 285
Martin D. C. et al., 2007, ApJS, 173, 342
Meier D. L., 2003, New Astron. Rev., 47, 667
Mushotzky R., 2004, Astrophys. Space Sci. Library, 308, 53
Nesvadba N. P. H., Lehnert M. D., De Breuck C., Gilbert A. M., van Breugel W., 2008, A&A, 491, 407
O'Dea C. P. et al., 2008, ApJ, 681, 1035
Oemler A., Dressler A., Kelson D., Rigby J., Poggianti B. M., Fritz J., Morrison G., Smail I., 2009, ApJ, 693, 152
Papadopoulos P. P., Kovacs A., Evans A. S., Barthel P., 2008, A&A, 491, 483
Pipino A., Kaviraj S., Bildfell C., Babul A., Hoekstra H., Silk J., 2009, MNRAS, 395, 462
Poggianti B. M. et al., 2009, ApJ, 693, 112
Quintero A. D. et al., 2004, ApJ, 602, 190
Rafferty D. A., McNamara B. R., Nulsen P. E. J., Wise M. W., 2006, ApJ, 652, 216
Reviglio P., Helfand D. J., 2006, ApJ, 650, 717
Rupke D. S., Veilleux S., Sanders D. B., 2005, ApJ, 632, 751
Salpeter E. E., 1955, ApJ, 121, 161
Sanders D. B., Mirabel I. F., 1996, ARA&A, 34, 749
Schawinski K., Thomas D., Sarzi M., Maraston C., Kaviraj S., Joo S. J., Yi S. K., Silk J., 2007, MNRAS, 382, 1415
Shabala S. S., Ash S., Alexander P., Riley J. M., 2008, MNRAS, 388, 625
Shin M.-S., Ostriker J. P., Ciotti L., 2010, ApJ, 711, 268
Shioya Y., Bekki K., 2000, ApJ, 539, L29
Shlosman I., Begelman M. C., Frank J., 1990, Nat, 345, 679
Sijacki D., Springel V., Di Matteo T., Hernquist L., 2007, MNRAS, 380, 877
Smith H. E., Lonsdale C. J., Lonsdale C. J., 1998, ApJ, 492, 137
Smolčić V., 2009, ApJ, 699, L43
Springel V., Di Matteo T., Hernquist L., 2005, ApJ, 620, L79
Tadhunter C., Robinson T. G., González Delgado R. M., Wills K., Morganti R., 2005, MNRAS, 356, 480
Tojeiro R., Heavens A. F., Jimenez R., Panter B., 2007, MNRAS, 381, 1252
Tojeiro R., Wilkins S., Heavens A. F., Panter B., Jimenez R., 2009, ApJS, 185, 1
Tongue T. D., Westpfahl D. J., 1995, AJ, 109, 2462
Tran K.-V. H., Franx M., Illingworth G. D., van Dokkum P., Kelson D. D., Magee D., 2004, ApJ, 609, 683
Tremblay G. R., O'Dea C. P., Baum S. A., Koekemoer A. M., Sparks W. B., de Bruyn G., Schoenmakers A. P., 2010, ApJ, 715, 172
Tremonti C. A., Moustakas J., Diamond-Stanic A. M., 2007, ApJ, 663, L77
Trichas M., Georgakakis A., Rowan-Robinson M., Nandra K., Clements D., Vaccari M., 2009, MNRAS, 399, 663
Vanden Berk D. E. et al., 2006, AJ, 131, 84
Veilleux S., 2001, in Tacconi L., Lutz D., eds, Proceedings of Starburst Galaxies: Near and Far, The Starburst–AGN Connection. Springer-Verlag, Heidelberg, p. 88
Vernaleo J. C., Reynolds C. S., 2006, ApJ, 645, 83
Wang R. et al., 2010, ApJ, 714, 699
Wills K. A., Tadhunter C., Holt J., González Delgado R., Inskip K. J., Rodríguez Zaurín J., Morganti R., 2008, MNRAS, 385, 136
Wilson A. S., Colbert E. J. M., 1995, ApJ, 438, 62
Yagi M., Goto T., Hattori T., 2006, ApJ, 642, 152
Yamauchi C., Yagi M., Goto T., 2008, MNRAS, 390, 383
Yan R., Newman J. A., Faber S. M., Konidaris N., Koo D., Davis M., 2006, ApJ, 648, 281
Yang Y., Tremonti C. A., Zabludoff A. I., Zaritsky D., 2006, ApJ, 646, L33
York D. G. et al., 2000, AJ, 120, 1579
Yun M. S., Reddy N. A., Condon J. J., 2001, ApJ, 554, 803
Zabludoff A. I., Zaritsky D., Lin H., Tucker D., Hashimoto Y., Shectman S. A., Oemler A., Kirshner R. P., 1996, ApJ, 466, 104

This paper has been typeset from a TEX/LATEX file prepared by the author.